PHYSICAL REVIEW B VOLUME 18, NUMBER 4 15 AUGUST 1978

Photoelectronic behavior of a-Se and some a-Se:As alloys in their glass transition regions

M. Abkowitz and D. M. Pai
Xerox Webster Research Center, Rochester, New York 14644
(Received 9 November 1977)

Coordinated measurements of dielectric response, hole and electron drift mobilities, photogeneration efficiencies, and space-charge-limited currents have all been carried out on a-Se and some a-Se:As alloys under experimental conditions in which temperature is continuously scanned at a preselected, constant rate over a range encompassing their respective glass transitions. In addition to the time-temperature profile of sample films during measurement, preparatory procedure and thermal history prior to measurement are also fixed. The single dielectric loss peak observed exhibits a temperature and frequency dependence in conformity with the phenomenological Williams-Landel-Ferry equation but the spectra recorded during the initial heating of a well-rested sample film are found to differ systematically from spectra obtained in subsequent scans carried out in a program of repeated thermal cycling experiments. This latter behavior is attributed to a fully reversible thermal hysteresis in molecular packing and its characteristic relaxation time is determined to be days at 294 K. The impact of this structural transition on photoelectronic behavior is readily identified, but is itself superimposed on the marked change in temperature dependence of drift mobility and photogeneration efficiency which is always found to accompany the glass-transition process. Two trapping phenomena also reflect the glass transition. The first is manifested at T_g as the sudden appearance of an abrupt range limitation on electron transport and is hysteresis-free on our experimental time scale. The second which shows a pronounced thermal hysteresis can be experimentally related to the fluctuation in molecular packing and is manifested as an abrupt drop in trap-limited space-charge-limited current during the first heating cycle through T_g.

I. INTRODUCTION

A. Background

During the isobaric cooling at a selected rate of a glass-forming liquid there is a temperature below which the rate of structural relaxation slows down sufficiently to cause the heat capacity and enthalpy to deviate from the values on an extrapolated equilibrium-liquid curve.[1] As the temperature is reduced still further to the "freeze-in" value structural relaxation essentially ceases on the experimental time scale. The temperature range bounded by these two temperatures is the glass-transition region. For a glass subjected during formation and before measurement to a specified time-temperature history one typically observes relatively abrupt changes in heat capacity, specific-volume enthaply, and compressibility at an experimental temperature in the glass-transition region which is taken to be the glass-transition temperature T_g. T_g depends on both the time-temperature history of the glass before and during measurement and the nature of the measurement itself. In practice, T_g is conveniently determined by differential scanning calorimetry where it is taken to be the intersection of the extrapolated liquid and glass enthalpy versus temperature curves during cooling at a specified rate, or the temperature of onset of a rapid increase of the isobaric heat capacity versus temperature during heating, or even the inflection temperature of the latter curve. Below the glass-transition region the amorphous solid is in a state of inhibited metastable equilibrium where only local-mode excitations can persist. In the glass-transition region the amorphous solid rapidly gains the freedom to undergo structural relaxation toward a thermodynamic state given by the extrapolated equilibrium-liquid curve. At the same time the molecules of the amorphous medium become free to participate in a collective type of persistent micro-Brownian motion the Fourier components of which can in part be resolved in dynamic mechanical measurements, and dielectric relaxation spectra. The latter thermally excited molecular motions characteristic of an amorphous medium above its glass-transition temperature are usually described in terms of a relaxation-time distribution function. The central relaxation time of this distribution is, for a large collection of glassy materials, found to vary with temperature according to a phenomenological equation constructed by Williams, Landel, and Ferry (WLF).[2] The more complicated temperature-dependent relaxation behavior described by the WLF equation is readily distinguished from local-mode behavior which is simply activated.

Both the thermodynamic parameters of a glass and the motional states of its constituent molecules change suddenly at the glass transition. It is reasonable to presume that a similar rapid

alteration of the density and distribution of electronic states may also be initiated. For example, the frozen-in population of charged defect species recently proposed to explain many of the electronic properties of chalcogenide glasses might vary according to the time-temperature history of a given specimen film near T_g.[3-7]

B. Scope

How the glass transition impacts the photoelectronic behavior of an amorphous semiconductor is clearly an issue of fundamental interest which both bears on our understanding of the microscopic electronic processes in that medium and at the same time furnishes a new set of experimental perspectives on the glass-transition process itself. We have measured the electron and hole drift mobilities, photogeneration efficiency, and one-carrier trap-limited space-charge-limited current in flash evaporated amorphous selenium films alloyed with up to several percent As as sample temperature was continuously scanned at a fixed rate over a range encompassing their respective glass transitions.[8] Dielectric relaxation spectra have been obtained in these flash evaporated films by synchronously detecting and continuously recording both components of the ac current at a preselected and fixed frequency as sample temperature was analogously scanned in the apparatus used for making photoelectronic measurements.[3] These measurements all lend themselves to direct comparison with dynamic mechanical and differential scanning calorimetry data both routinely carried out in a temperature scan mode. Experimental parallels of this kind are advantageous when measuring phenomena which can reflect the time-temperature profile of the sample specimen.

II. EXPERIMENTAL

Amorphous films were prepared by flash evaporation at 10^{-6} Torr of a charge of the appropriate 99.999% purity starting material onto an aluminum substrate held at the respective glass-transition temperature to assure vitrification. Homogeneity of the arsenic profile in representative films was verified using energy dispersive x-ray analysis. X-ray photoemission spectroscopy indicates that any chemically incorporated oxygen is below the detectable limit (0.1-at.% monolayer). The absence of room-temperature ESR in these films precludes both paramagnetic oxygen-selenium charge transfer states and the organoselenium radical complexes which sometimes appear as a contaminant in selenium source material that has been stored in polyethylene containers.[9]

All electrical measurements were made on sandwich-type cell structures formed by vacuum depositing a semitransparent gold electrode on the top surface of the film. In measuring carrier mobilities by the time-of-flight technique the transit of a carrier packet generated near the top surface by a strongly absorbed light flash is time resolved as it drifts across the sample thickness under a uniform applied field.[10] When the measurements are made in the current mode the time constant of the current sensing circuit is made shorter than the transit time. Though quantum efficiency of photogeneration can be calculated from the product of transit time and current pulse height it is generally more accurate, particularly in dispersive transport media, to make the latter measurements in a voltage mode configuration. In this configuration one electronically integrates the total charge in transit by making the sensing circuit time constant much larger than a typical transit time.[11] Sample temperature was varied continuously at a chosen rate in these measurements using a programmable environmental test chamber. Dielectric relaxation spectra were obtained by measuring synchronously both components of the ac current developed in a series circuit containing the sample, an oscillator, and an operational amplifier.[12] The operational amplifier converts the complex current to a complex voltage which is detected using a two-channel lock-in amplifier and then recorded as the temperature is scanned under conditions identical to those used in making photogeneration and transport measurements. Frequency, the parametric experimental variable, could be varied from 0.3 to 10^6 Hz. When these ac measurements are augmented by thermally stimulated depolarization[12] it becomes possible to characterize the molecular dynamic process at T_g over a nine order range in relaxation time. Space-charge-limited currents sustained by a light generated contact were recorded using a logarithmic picoammeter as sample temperature was scanned though T_g in the apparatus common to the other measurements. The light source was the 4416 Å line of a helium-cadmium laser.

III. RESULTS

A. Time-temperature profile

All measurements were carried out using a programmable temperature chamber in which temperature stability and uniformity could be electronically maintained to within 1 K at the sample fixture. Temperature uniformity over the working space was monitored using an array of thermocouples and platinum resistance thermo-

meters, some of which were always kept in direct thermal contact with the sample film. Unless otherwise noted the temperature scanning program was standarized to the following.

(i) A series of scans would be initiated on a film only after it had first been stored for at least three days at 294 K (room temperature). This annealing procedure was also necessary after initial fabrication of the sample film by flash evaporation onto a substrate held at T_g. The effect of more extended room-temperature annealing on all the measurements reported was however also investigated.

(ii) A sample film is first rapidly cooled to a starting temperature below 250 K and then heated at a fixed 4 K/min rate to about $T_g + 20$ K while the experimental parameter of interest is recorded. The sample is then cooled at 10 K/min to the starting temperature to complete the first thermal cycle. Data is usually recorded only during the heating step. Subsequent cycles are run under otherwise identical conditions but our ability to obtain multiple heating cycle data is limited by an increase, after many heating cycles above T_g, in film microcrystallinity. With repeated thermal cycling one can, for example, begin to detect a progressive increase in the free-electron contribution to low-frequency dielectric dissipation long before there is any textural or visual indication of film degradation.

(iii) First cycle measurements of dielectric relaxation, drift mobilities, photogeneration efficiency, and space-charge-limited currents are found to all exhibit unique and correlated features which do not reappear in subsequent thermal cycles carried out during the same nominal laboratory day. These latter features can however be fully reproduced after the sample film is annealed at 294 K for several days. Data recorded during the second thermal cycle is identical to the data obtained thereafter in multiple cycling experiments except for effects clearly associated with progressive film degradation. The structural origin of the changes in photoelectronic behavior induced during the first thermal cycle of a sample film is more directly discerned by analyzing the corresponding effects observed in dielectric relaxation spectra.

B. Dielectric relaxation spectra

A single dielectric relaxation is detected between 170 and 340 K in a-Se and in a-Se:As alloy films containing up to several percent As. The relaxation can be unambiguously assigned to the glass-transition process because of its proximity to the glass-transition temperature measured

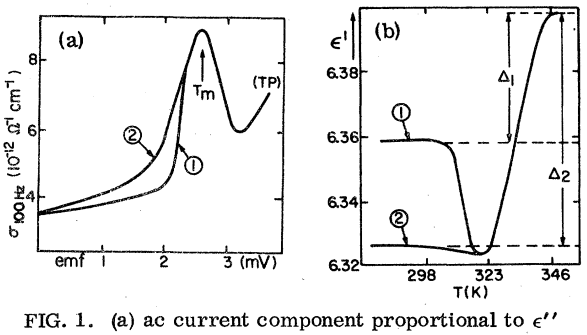

FIG. 1. (a) ac current component proportional to ϵ'' represented as ac conductivity vs emf of a copper-constantan thermocouple. 100-Hz 10-mV rms bias TP denotes maximum temperature, during heating cycle. TP ≡ turning point. Trace 1 is first thermal cycle of a-Se sample dark rested for days at 295 K. Trace 2 represents subsequent cycles recorded during same nominal 8 hour period and shows no thermal hysteresis at 4 K/min scanning rate. (b) ϵ' vs T (K) from ac current measurement on above samples Δ_1 and Δ_2 are dielectric increments of relaxation corresponding to traces 1 and 2. Curve 1, in Figs. 1(a) and 1(b), is reproduced when film previously heated above T_g is stored at 294 K for several days in dark. emf and T(K) scales are equivalent.

calorimetrically at the same thermal scanning rate, its shift to higher temperature at a given frequency with As doping,[13] and its overall temperature and frequency-dependent behavior which we have demonstrated to be of the WLF type and not the Arrhenius-type.[2] While the position of the dielectric loss peak is insensitive to thermal scanning rate at a fixed frequency the overall shape of the spectra are found to be systematically dependent on the sample films' thermal history. In Fig. 1(a) current trace (1) is recorded using 100-Hz 10-mV bias during the first thermal cycle of an a-Se sample film. The low-temperature truncation of the loss peak was an experimental characteristic not only of a-Se but of all the Se:As alloy films during their first heating cycle. Current trace (2) is the next scan run under identical conditions and no longer shows the original truncation. All subsequent thermal scans are essentially identical to trace (2) if they are carried out in the same nominal time frame (i.e., laboratory day). After the sample has been annealed for several days at 294 K, however, trace (1) is again reproduced during the first heating cycle of the film. Analogous behavior of the sample capacitance represented as an effective dielectric constant is shown in Fig. 1(b), traces (1) and (2). Δ_1 and Δ_2 are the corresponding dielectric increments of the relaxation and are defined in Fig. 1(b). The reduction in room-temperature effective dielectric constant observed after completion of the first heating cycle is again a char-

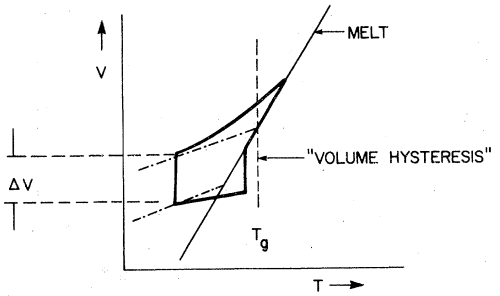

FIG. 2. Isobaric V vs T plot schematically illustrates volume hysteresis effect. Melt curve which applies to the liquidlike region well above T_g is unique. Alternate dash and dotted curves represent amorphous solid below T_g in inhibited metastable equilibrium with the lower lying curve representing the more densified or relaxed glass. ΔV is the volume increment of the structural relaxation. Solid curves represent experimental time temperature history of sample film. Lower portion of loop, from left to right, describes cycle 1 behavior (see text).

acteristic of the entire system of alloy films studied. The relaxation to the original room-temperature dielectric constant is essentially completed on a time scale of days if the sample is allowed to anneal at 294 K. Our explanation for this cyclic and thermal history dependent behavior in dielectric parameters is depicted schematically in Fig. 2. The underlying phenomenon is volume hysteresis, a fully reversible but relatively slow relaxing variation in molecular packing.[1] On originally cooling the melt below T_g, the sample exhibits a temperature-dependent specific volume given by the upper glass curve on the V-T diagram. Left to anneal at 294 K the glass slowly densifies, suffering a reduction in volume ΔV as indicated. If the glass is reheated toward T_g, its temperature-dependent volume is now given by the lower glass curve on the V-T plot. Depending on the heating rate there will typically be some overshoot of the extrapolated melt curve during the initial heating cycle. This behavior is followed by a relatively precipitous increase in the loss peak during first heating of our relaxed films and an equally precipitous and corresponding decrease in the sample's effective dielectric constant which is really measuring a decrease in packing density in the film plane. For these films which are typically 10 μm thick the fluctuation in thickness as a result of these processes is estimated to be about 0.5% if one neglects any accompanying change in the average molecular polarizability. It should be emphasized that volume hysteresis with its very long relaxation time is superimposed on the Fourier components of the molecular motional processes whose much faster relaxations are being directly measured in these experiments. In fact, the loss peaks themselves exhibit no significant thermal hysteresis (i.e., do not shift) in the scanning experiments, at least in the audio-frequency range as temperature sweep rates are changed. During the second and all subsequent thermal cycles the glassy film will remain in its less dense state as depicted by the upper glass and melt curves on the schematic V-T diagram. The latter underlies our observation of an invariance in the dielectric spectra after completion of the second thermal cycle in a program of repeated cycling experiments. A volume hysteresis phenomenon in our sample films can also be inferred from an analysis of scanning calorimetry data.

C. Transport

Hole drift mobilities were measured by the time of flight technique as the temperature was scanned continuously at 4 K/min. In Fig. 3 open circles, squares, and triangles are data collected on several Se:0.3-at.%-As alloy films during thermal cycle (1). Solid circles are recorded during the second thermal cycle and in complete analogy to the second cycle behavior of the dielectric relaxation spectra will continue to reproduce in all subsequent thermal cycles if they are carried out during the same laboratory day. Allowing the sample to anneal at 294 K for several

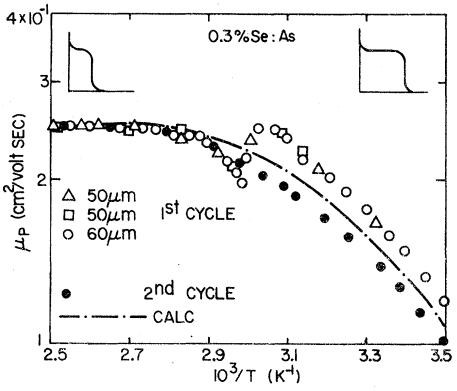

FIG. 3. Log hole drift mobility vs $10^3/T$ at 10^5 V/cm for 0.3-at.%-As doped selenium films. Open triangles, squares, and circles are measured during first thermal cycle of film previously stored at 295 K for days. Solid circles are subsequent thermal cycles. Calculated curve based on shallow-trap model taking $E_p = 0.247$ eV. (See concluding remarks in text.) Inserts illustrate that hole transit shapes remain unchanged on passing through the glass transition.

days after the last heating cycle has been completed however fully restores cycle (1) behavior. The reduction in drift mobility values at temperatures below the glass transition observed during the second and all subsequent thermal cycles is larger than can be accounted for simply on the basis of an accompanying 0.5% change in the film's thickness.

The concentration of As in these films can be varied in the 0%–2% range without producing any deviation from either hole transport behavior, illustrated in Fig. 3 for temperatures below the glass transition, or from the saturated value of the drift mobility, above the glass transition. In the nominal 1-at.%-As concentration range the shape of the hole transits retain their nondispersive shape and are thus not affected as temperature is swept through the glass-transition region. The corresponding transit pulse shapes become dispersive, however, at very low temperatures. Room-temperature hole transits do become dispersive and ultimately lifetime limited as As concentration is increased beyond 2 at.%.[14] The increasingly dispersive hole transit pulse shape observed below the glass transition as As concentration is increased makes it more difficult to resolve the small changes in transit time observed in the glass-transition region during the first thermal cycle. It is for this latter reason and not because of a lifetime limitation that we have somewhat arbitrarily restricted our hole drift mobility measurements to alloy films in which As concentration does not exceed 1 at.%. Figure 3 illustrates an extensive region above the glass transition for which the temperature dependence of the hole drift mobility has become saturated. At the highest temperatures indicated on Fig. 3 the glass begins to soften and suffer other irreversible morphological changes. For our present purposes the experimental temperature range was usually restricted to allow us to establish reproducibility of the measurements under repeated cycling.

Temperature-dependent drift mobility data for electrons is compared in Fig. 4 for amorphous selenium and for a 3-at.%-As containing Se:As alloy film. Open circles represent the data collected during the first thermal cycle and the solid circles describe results obtained for the subsequent cycles. Cycle (1) behavior is restored by room-temperature annealing for several days just as it is for hole transport. Hole transport becomes temperature independent in the glass-transition region with no accompanying shape change in the transit pulses whereas electron transport becomes abruptly lifetime limited. The onset of a range limitation for electrons at

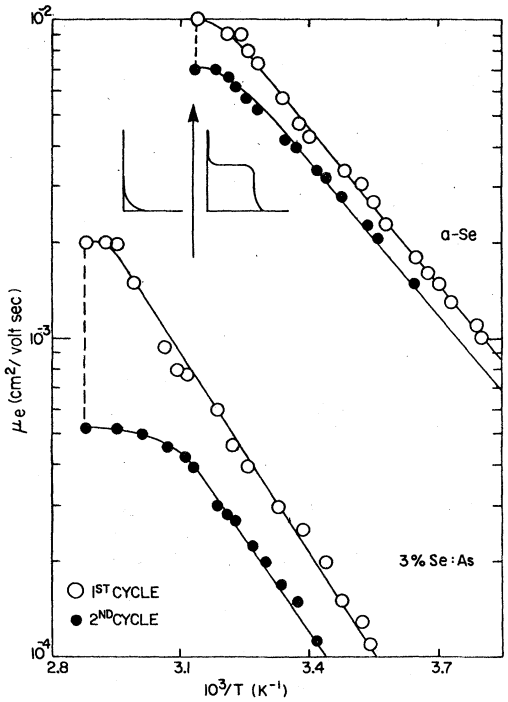

FIG. 4. Log electron drift mobility versus $10^3/T$ at 10^5 V/cm for *a*-Se and a 3-at.%-As containing Se:As alloy film. Open circles are measured during first thermal cycle of film previously stored in 294 K for days. Solid circles are subsequent thermal scans (see text). Dashed line depicts drop in mobilities just preceding onset of range limited transport. Inserts depict transit pulse below T_g and lifetime limited signal above T_g.

the glass transition is schematically illustrated by the inserts which represent the associated transient current response that is measured in each temperature region. During the first thermal cycle one can always resolve an abrupt drop in electron mobility which just precedes the onset of the range limitation. The depressed values of electron mobility then continue to be reproduced under repeated thermal cycling at temperatures below the glass transition. Both electron and hole drift mobilities are thus seen to exhibit a similar thermal hysteresis which we have demonstrated derives directly from a microscopic manifestation of the volume hysteresis effect, i.e., is much larger than can be accounted for simply on the basis of sample expansion. Electron and hole drift mobilities in the Se:As alloys exhibit significantly differing behavior in other important respects. For example, Fig. 4 illustrates the sensitivity of electron drift mobility to As doping.[14,15] For electrons below the glass transition the transit pulses remain nondispersive even as As content increases in the alloy films. It is therefore

possible for us to clearly illustrate that the demarcation in transport behavior with increasing temperature occurs at the glass transition and as a result is expected to shift to higher temperatures with increasing As content. The overriding temperature-dependent feature which is common to both carriers but which is obscured to some extent by the onset of a lifetime limitation for electrons is a change from activated behavior below the glass transition to a saturated behavior above it. After the first thermal cycle has been completed one can pass repeatedly from the activated to saturated transport behavior and back without observing any thermal hysteresis in mobility values as temperature is varied through T_g. On the other hand, the drop in electron and hole mobilities observed only during the first thermal cycle through T_g is superimposed on this behavior.

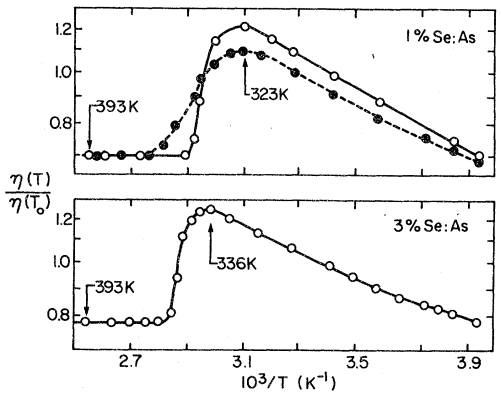

FIG. 5. Log quantum efficiency normalized to its absolute value at 294 K vs $10^3/T$ for two alloy samples. $E=10^5$ V/cm, $\lambda=450$ nm. Open and solid circles represent thermal cycle 1 and all subsequent cycles recorded during same 8-h period, respectively. Cycle 1 data, open circles, reproduce when film previously heated above T_g is then stored at 294 K for several days in dark. Overall transition from activated behavior below T_g to temperature independence above T_g, however, shows no thermal hysteresis at 4 K/min scanning rate. Note that sharp transition region in cycle 2 is broadened during thermal cycle 2. Compare with onset of glass-transition process measured dielectrically and shown in Fig. 1 for cycles 1 and 2.

D. Photogeneration

In Fig. 5 the quantum efficiency of supply for holes in amorphous Se:As alloy films containing 1-at.% and 3-at.% As are compared. These measurements were made as sample temperature was continuously scanned at 4 K/min. Quantum efficiency data shown in Fig. 5 has been normalized to its value at 294 K. Quantum efficiency of supply for holes is the number of holes per incident photon exiting a thin region of the sample in which all of the incident light is absorbed. Surface recombination and surface trapping makes the supply efficiency smaller than the absolute quantum efficiency of photogeneration. At an excitation wavelength of 4500 Å and a field of 10^5 V/cm the supply efficiency for holes at the reference temperature of 294 K is 0.3. Penetration depth for the 4500 Å illumination is 0.1 μm. Flash evaporated films were 10 μm thick. Quantum efficiencies were measured by time-of-flight voltage mode experiments at a field of 10 V/μm. It is important to be able to demonstrate that all the charge released from the generation region is integrated which means, in particular, that no charge is lost to deep traps in the bulk of the sample being measured. It is known, for example, that hole lifetimes can vary considerably from sample to sample. One can independently determine whether lifetime effects intrude in the sample under study at the field used in the measurement by employing a xerographic technique. In the xerographic measurement the film is first corona charged to a positive polarity and then photodischarged using the highly absorbed 4500-Å radiation. The photogenerated holes transit the sample without any loss due to bulk trapping as long as their transit time (T_t) remains much shorter than their lifetime against deep trapping (τ_{tr}). As the film discharges the transit time increases and this process continues until the transit time approaches τ_{tr} at which point a fraction of the photogenerated carriers begin to fall into deep traps. In this limit is can easily be shown that the residual potential corresponding to the field at which $\tau_{tr}=T_t$ is given by $V_R \approx L^2/\mu T_t$, where L is the film thickness and μ the hole drift mobility. On a time scale defined by the initial rate of photodischarge the residual potential can be regarded as constant. Even our 10-μm films containing 3-at.% As when charged to an initial electric field of 10^5 V/cm were found to discharge to a residual field of $\sim 3\times 10^4$ V/cm. On this basis we are able to conclude that photogeneration measurements carried out at 10^5 V/cm were not perturbed by bulk trapping effects.

In Se it has been established that the hole quantum efficiency of supply is the true quantum efficiency at 10 V/μm though at lower fields one detects a quantum efficiency of supply perturbed by surface recombination/trapping.[16] We did not attempt to measure the field dependence further because of the narrow experimental window bounded by a range limitation below 3×10^4 V/cm and electrical breakdown of our films at a field in excess of 10^5 V/cm when temperature exceeded

T_g.

During the first heating cycle an abrupt drop in normalized photogeneration efficiency is observed in the glass-transition region. It is clear from Fig. 5 that this drop occurs at progressively higher temperatures as the As content, and thus the glass-transition temperature, increases. Photogeneration efficiency exhibits thermally activated behavior below T_g but abruptly decreases and then becomes temperature independent above T_g. During the second or any subsequent thermal cycle both a decrease in generation efficiency and a simultaneous transition from activated to temperature-independent photogeneration efficiency still persist. There is, however, no longer any thermal hysteresis in the measurement even when the sample is repeatedly cycled through T_g at 4 K/min in either direction. It is evident in Fig. 5 that the decrease in photogeneration efficiency in the glass-transition region preceeding the onset of temperature-independent behavior takes place over a broader temperature range during the second thermal cycle. The transition in behavior of the photogeneration efficiency evidently provides a sensitive mapping of the onset of the glass-transition process closely paralleling features observed in the dielectric relaxation spectra.

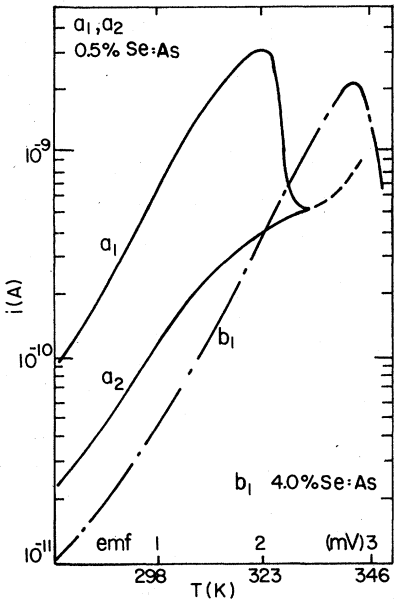

FIG. 6. One carrier SCLC sustained by continuous surface illumination (4416-Å laser) vs T (K). $A = 0.34$ cm^2, $d = 122\,\mu$m, 10 V applied. a_1 and a_2 are the first and second thermal cycle behavior of 0.5-at.%-As doped selenium film (as defined previously), b_1 is first thermal cycle of 4-at.% As in Se film. a_1 is reproduced when film previously heated above T_g is stored at 294 K for several days in the dark.

E. Space-charge-limited currents (SCLC)

Any change in deep trapping associated with the glass transition could be detected by either a direct measurement of carrier lifetime using the time of flight technique or alternatively by a measurement of trap-limited SCLC. In the time-of-flight measurement one discerns lifetime from the characteristic shape change of the transit pulse as the applied field is reduced to a threshold value for which carrier transit time becomes the lifetime against a trapping event. Such a shape change is difficult to identify when well-defined transits are not observed even in the absence of a lifetime limitation at temperatures well below T_g. This is in fact the situation that prevails for hole transport in our alloy films containing more than 0.5-at.% As. The requirement for observation of SCLC is that an Ohmic reservoir of carriers exists to sustain the current at field for which the carrier transit time is of the order of a Maxwellian relaxation time. Pfister and Lakatos[17] have demonstrated that SCLC can be sustained in amorphous selenium films at room temperature by a photogenerated contact. In the high surface photoexcitation limit where the one carrier injection currents become light intensity independent they found the steady-state hole current to be almost six orders of magnitude smaller than would be estimated by using the measured hole drift mobility value 0.14 cm^2 V^{-1} sec^{-1} suggesting that deep trapping effects modify the SCLC. Our measurements on Se:As alloy films fully parallel the results reported by Pfister and Lakatos at 294 K but are also carried out as temperature is continuously scanned through T_g at 4 K/min. In our apparatus, steady intense surface absorbed irradiation was provided by a 100-MW 4416-Å laser. Light intensity independence of the current was verified over the entire temperature range. Typical current traces are shown in Fig. 6. On initially irradiating a dark rested sample at 294 K the current is many orders of magnitude larger than its eventual steady-state value. The time required after irradiation is applied to achieve a current level within a factor 2–3 of the final value is about 30 sec. Trace a_1 in Fig. 6 is the current recorded logarithmically during the first thermal cycle of an Se:As alloy film containing 0.5-at.% As at a 4-K/min scanning rate while the sample is continuously irradiated. The activation energy of the current between 273–320 K is approximately 0.43 eV whereas the activation energy of the hole drift mobility alone is 0.14 eV.[18] In the simplest

picture the deficit would represent a trap lying approximately 0.3 eV above the transport states. Traces a_1 and b_1 allow us to compare the first thermal cycle hole injection currents for a-Se films containing 0.5-at.% and 4-at.% As, respectively. The injection current levels below T_g decrease with increased As doping so that the current density at 294 K is about an order of magnitude smaller in the 4-at.%-As doped film than in the film doped with only 0.5-at.% As. We see directly that As introduces hole traps. Activation energy below T_g is apparently insensitive to As concentration. Above T_g dark generation increases rapidly becoming comparable to the rate of injection from the illuminated surface. During the first thermal cycle the injection current is observed to drop about a factor of 5 in the glass-transition region. The current levels remain depressed as indicated during the second and all subsequent thermal scans carried out during the same laboratory day. Cycle 1 behavior is restored by a dark rest at 294 K for several days. The drop in injected current near T_g can therefore be clearly associated with the volume hysteresis phenomenon. The magnitude of the drop in injected current near T_g during thermal cycle 1 is four times larger than the drop we measure in hole drift mobility and must therefore primarily reflect an abrupt increase in trap population. The activation energy of the SCLC does not appear to change however from thermal cycle 1 to thermal cycle 2 even as the current level drops sugesting that the traps being created are not an entirely new structural species rather that the fluctuation occurs in a trap population normally resident in the glass.

IV. DISCUSSION AND CONCLUDING REMARKS

(i) Dielectric relaxation measurements carried out in an apparatus in which the sample film is subjected to a programmed thermal history during measurement allow us to separately resolve two features of the glass-transition process in amorphous Se and Se:As alloy films. Temperature and frequency dependence of the single loss peaks observed allow us to characterize the underlying molecular relaxation process. Like many amorphous solids the relaxation process at the glass transition in a-Se:As alloys is not simply activated but instead conforms to the phenomenological WLF equation. The underlying kinetic process is believed to involve large scale molecular configuration rearrangements having some cooperative character. Superimposed on the latter process is a fully reversible thermal hysteresis in molecular packing. Thermal cycling and long term room-temperature annealing experiments demonstrate that after a heating cycle through T_g the films take days at 294 K to redensify. These processes clearly impact photoelectronic behavior. To systematize that impact we have measured transport, photogeneration and trapping under programmed time temperature conditions which facilitate direct comparison with dielectric and scanning calorimetry data.

(ii) Though hole and electron drift mobilities in a-Se:As alloys are distinctive in many important respects below T_g, their general behavior with respect to the glass-transition process as perceived in our thermal cycling experiments is surprisingly similar. Both drop abruptly near T_g during the first thermal scan and both evolve from a thermally activated temperature dependence below T_g to a temperature-independent (saturated) value above T_g. Saturation of the temperature dependence of the hole drift mobility is apparent in Fig. 3 but for the case of electrons is truncated by the onset of a lifetime limitation above T_g. Both electron and hole drift mobilities remain depressed below T_g during the second and all subsequent thermal scans measured in a program of repeated thermal cycles. By studying the rate of recovery of drift mobilities below T_g to their "rested" values we establish that the experimental features of transport unique to the first thermal cycle parallel the volume hysteresis phenomenon i.e., first cycle fluctuation in drift mobility reflects fluctuation in the molecular packing. We cannot definitively establish, however, whether variation in molecular packing directly impacts intersite charge transfer efficiency or whether its effect is manifested through a resulting variation in an interactive shallow-trap population. In this connection the applicability of the shallow-trap controlled drift mobility model to selenium has itself been called into question by recent experimental results of Juska *et al.*[19] and Pfister.[20] Juska *et al.* have compared the temperature dependencies of hole drift mobility, dc conductivity, and thermopower in bulk quenched selenium samples. They found that subtracting the activation energy of the hole density compiled from their thermopower measurements, from the dc conductivity activation energy yielded an activation energy identical to that obtained from their hole drift mobility measurements. Based on this observation they argue that the hole drift mobility is the microscopic mobility, i.e., transport is not influenced by interaction of drifting charge with traps. Pfister has studied hole drift mobility down to 77 K. At room-temperature hole transit pulses exhibit a rectangular shape indicating that there is little dispersion of the carrier sheet, however, at low-temperature transit pulse shapes do be-

come very dispersive. It would be natural to propose a transition from trap controlled band transport to transport by hopping among the shallow states as temperature is lowered but there is no evidence for a change in transport activation energy, i.e., no evidence for a change in the mechanism of carrier motion. The latter observation is not simply[21] reconciled with a trap controlled band transport model. The latter issue is relevant to us here for the following reason: without taking account of the glass-transition phenomenon at all we can calculate the shallow-trap controlled drift mobility for holes using the expression[21]

$$\mu_p = \mu_{0p}[1 + (N_{tp}/N_v)\exp E_p/kT]^{-1},$$

where μ_{0p} is the microscopic mobility and N_{tp}/N_v the ratio of shallow-trap to valance-band density of states, E_p is the trap depth. The dashed curve in Fig. 3 is calculated taking $E_p = 0.247$ eV, assuming an effective density of valence-band states proportional to $T^{3/2}$ and a microscopic mobility controlled by lattice scattering. The choice of adjustable parameters is determined by best fitting the expression for μ_p to low-temperature data. On this basis we obtain for the room-temperature microscopic mobility 0.44 $cm^2/V^{-1}sec^{-1}$. The latter is close to the value obtained by Grunwald and Blakney[22] who applied a similar analysis to their amorphous selenium data. Clearly, the dashed curve predicts a broad peak in drift mobility in the region where the experimental value is observed to saturate. To the extent then that the shallow-trap controlled picture remains a viable model for hole transport in these materials and because of the fact that hole transit data is limited in this study to those samples containing 1-at.% As or less we are not able to conclude that saturation of the hole drift mobility is solely a reflection of the glass-transition process. Variation in As concentration does provide an opportunity to study the effect of modulating the glass-transition temperature. It is significant particularly in the above context that the glass transition can be experimentally identified as the demarcation region for saturation of the electron drift mobility. The latter is a consequence of our ability to record electron transits in alloy films containing up to 5-at.% As. The abrupt drop in first cycle drift mobility observed for both carriers over a narrow temperature range near T_g can however be observed to shift with T_g even for holes.

(iii) Transport above the glass transition but below the crystalline melting point for selenium appears to differ decidedly from transport behavior reported for the melt[19] which is again activated with approximately twice the activation energy exhibited by the amorphous solid at low temperature, and if extrapolated into the corresponding temperature range hole mobilities in the melt would be orders of magnitude smaller than the saturated drift mobility actually measured in the amorphous solid above its T_g.

(iv) A tendency toward saturation of the hole drift mobility above T_g at a value close to that reported here has also been reported in bulk quenched selenium glass samples.[19] The magnitude and temperature-dependent behavior of hole transport above T_g does not therefore appear to vary critically with the method used to form the amorphous solid.

(v) It has been established[16] that the Onsager mechanism can account for the field, temperature, and wavelength dependence of the photogeneration efficiency in amorphous selenium below T_g. The same model appears to be applicable to the low As containing alloy films described in this study. In the Onsager picture of photogeneration an incident photon creates a thermalized hole-electron pair. The carriers are initially separated by a distance r_0 which is strongly wavelength, but weakly temperature, dependent. The disassociation efficiency of the hole-electron pair reflects the competition between their mutual Coulomb attraction and the externally applied electric field. The carriers are presumed to undergo Brownian motion and their average mutual separation and individual trajectories are thus described by a diffusion equation. Since the starting point in the Onsager calculation is the thermalized carrier pair, the transport process by which the carriers arrive at their initial separation r_0 is not treated. An abrupt change in density of transport states, shallow traps, or intersite transfer efficiencies could easily be imagined to influence the r_0 and hence impact the photogeneration process. Yet a transition to fully temperature-independent behavior with a photogeneration efficiency saturated at a value substantially less than one cannot, we suspect, be easily rationalized on the basis of the Onsager or any other existing model.

(vi) We have been able to identify two distinct trapping phenomena which reflect the glass-transition process. The drop observed in trap-limited SCLC in the glass-transition region has been interpreted as indicating an increase in what is probably already a resident trap species. The density of these traps is increased during the first heating cycle and then anneals over a period of days to its long term value at a rate which parallels room-temperature densification of the glassy film after first heating, in other words, shows marked thermal hysteresis. The other trapping

phenomenon is reflected in the onset of a range limitation for electrons in the glass-transition region. It should be emphasized by way of contrast that this range limitation disappears when the glass is cooled below T_g. The onset and cessation of a lifetime limitation in fact persists for an indefinite number of thermal cycles and one detects no thermal hysteresis in this behavior beyond the time nominally required to establish thermal equilibrium.

[1]R. N. Haward, *Physics of Glassy Polymers* (Wiley, New York and Toronto, 1973), p. 5, and references therein.

[2]M. L. Williams, R. F. Landel, and J. D. Ferry, J. Am. Chem. Soc. 77, 3701 (1955).

[3]M. Abkowitz and D. M. Pai, Phys. Rev. Lett. 38, 1412 (1977).

[4]M. Kastner, D. Adler, and H. Fritzsche, Phys. Rev. Lett. 37, 1504 (1976).

[5]R. A. Street and N. F. Mott, Phys. Rev. Lett. 35, 1293 (1975).

[6]N. F. Mott, Philos. Mag. 34, 1101 (1976).

[7]P. W. Anderson, Phys. Rev. Lett. 34, 953 (1975).

[8]M. Abkowitz and D. M. Pai, *Proceedings of the Seventh International Conference on Amorphous and Liquid Semiconductors, Edinburgh, Scotland, 1977* (Center for Industrial Consultancy and Liaison, University of Edinburgh, 1977).

[9]M. Abkowitz, J. Chem. Phys. 46, 4337 (1967).

[10]W. E. Spear, Proc. Phys. Soc. Lond. B 70, 669 (1957); J. Mort, Phys. Rev. 5, 3329 (1972).

[11]D. M. Pai and S. W. Ing, Phys. Rev. 173, 729 (1968).

[12]M. Abkowitz and G. Pfister, J. Appl. Phys. 46, 2559 (1975).

[13]M. B. Myers and E. J. Felty, Mater. Res. Bull. 2, 535 (1967).

[14]J. Schottmiller, M. Tabak, G. Lucovsky, and A. Ward, J. Non-Cryst. Solids 4, 80 (1970).

[15]D. M. Pai, *Proceedings of the Fifth International Conference on Amorphous and Liquid Semiconductors, Garmisch Partenkirchen, 1973* (Taylor and Francis, London, 1974), p. 357.

[16]D. M. Pai and R. C. Enck, Phys. Rev. 11, 5163 (1975); R. C. Enck, Bull. Am. Phys. Soc. 211, 19 (1974).

[17]G. Pfister and A. Lakatos, Phys. Rev. B 6, 3012 (1972).

[18]J. L. Hartke, Phys. Rev. 125, 1177 (1962).

[19]G. Juska, S. Vengris, and J. Viscakas, in Ref. 15, p. 363; S. A. Vangris, Yu. K. Vishchakas, A. P. Sakalas, and G. B. Yushka, Soviet Physics Semiconductors 6, 903 (1972); G. Juska and S. Vengris, Phys. Status Solidi 16, K27 (1973).

[20]G. Pfister, Phys. Rev. Lett. 36, 271 (1976); G. Pfister and R. C. Enck, *Photoconductivity and Related Phenomena*, edited by J. Mort and D. M. Pai (Elsevier, Amsterdam, 1976) Chap. 7, p. 276.

[21]See, for example, J. Noolandi, Bull. Am. Phys. Soc. 22, 434 (1977); and F. W. Schmidlin, Phys. Rev. 16, 2362 (1977).

[22]R. M. Blakney and H. P. Grundwald, Phys. Rev. 159, 664 (1967).